European Journal of Medicinal Chemistry 118 (2016) 208–218

Contents lists available at ScienceDirect

European Journal of Medicinal Chemistry

journal homepage: http://www.elsevier.com/locate/ejmech

Research paper

Design, synthesis and biological evaluation of PSMA/hepsin-targeted heterobivalent ligands

Milan Subedi [a, 1], Il Minn [b, 1], Jianbo Chen [a, 1], YunHye Kim [a], Kiwon Ok [a], Yong Woo Jung [a], Martin G. Pomper [b], Youngjoo Byun [a, b, c, *]

[a] College of Pharmacy, Korea University, 2511 Sejong-ro, Jochiwon-eup, Sejong 339-700, South Korea
[b] Department of Radiology, Johns Hopkins Medical Institutions, 1550 Orleans Street, Baltimore 21287, MD, USA
[c] Biomedical Research Center, Korea University Guro Hospital, 148 Gurodong-ro, Guro-gu, Seoul 152-703, South Korea

ARTICLE INFO

Article history:
Received 4 January 2016
Received in revised form
14 March 2016
Accepted 12 April 2016
Available online 14 April 2016

Keywords:
PSMA
Hepsin
Prostate cancer
Heterobivalent ligands
Molecular imaging

ABSTRACT

Cell surface biomarkers such as prostate-specific membrane antigen (PSMA) and hepsin have received considerable attention as targets for imaging prostate cancer (PCa) due to their high cell surface expression in such tumors and easy access for imaging probes. Novel amidine-containing indole analogs (**13**–**21**) as hepsin inhibitors were designed and synthesized. These compounds showed *in vitro* inhibitory activity against hepsin with IC_{50} values from 5.9 to 70 μM. Based on the SAR of amidine-derived analogs, the novel heterobivalent compound **30**, targeting both hepsin and PSMA, was synthesized by linking compound **18** with Lys-urea-Glu, the key scaffold for the specific binding to PSMA, followed by the conjugation of the optical dye SulfoCy7. Compound **30** exhibited inhibitory activities against PSMA and hepsin, with IC_{50} values of 28 nM and 2.8 μM, respectively. *In vitro* cell uptake and preliminary *in vivo* optical imaging studies of **30** showed selective binding and retention in both PSMA and hepsin high-expressing PC3/ML-PSMA-HPN cells as compared with low-expressing PC3/ML cells.

1. Introduction

Prostate cancer (PCa) is the most common cancer in American men and the second leading cause of cancer death in this group [1]. The American Cancer Society estimates that there were approximately 220,800 new cases of PCa and 27,540 deaths from PCa in 2015 (www.cancer.org). The current gold standard for diagnosis of PCa is an elevated level of prostate-specific antigen (PSA) and abnormality of the prostate by digital rectal examination (DRE), followed by prostate needle biopsy [2]. However, benign conditions such as prostatitis and benign prostatic hyperplasia (BPH) can increase the level of PSA [3]. A comprehensive clinical study in Europe reported that PSA screening can lower the death risk from PCa, while a US study showed no statistical difference following PSA screening [4–6]. 76% of patients with a raised PSA level are not diagnosed with PCa, and 2% of patients with fast-growing PCa have a normal level of PSA (www.prostatecanceruk.org). Conversely, the effectiveness of DRE depends on the skill and experience of the examiner. 72–82% of individuals who undergo biopsy based on DRE findings are not diagnosed with PCa [7]. Therefore, there is an urgent need to explore novel biomarkers for the precise and efficient detection of PCa. Cell surface biomarkers including prostate-specific membrane antigen (PSMA), hepsin, and integrin-$\alpha_v\beta_3$ have received substantial attention as target proteins for the imaging of PCa due to their elevated cell surface expression on cancer cells compared with normal cells and easy access for imaging probes [8–14].

PSMA, a type II zinc-dependent protease, is highly expressed on the surface of prostate cancer cells as well as on the neovasculature of most solid tumors [15]. The active site of PSMA consists of two distinct sub-pockets, which form a 'glutarate-sensor' S1 site (pharmacophore) and an amphiphilic S1 site (non-pharmacophore). A cylindrical ~20 Å deep tunnel region exists adjacent to the S1 site and projects towards the hydrophilic surface of the enzyme

* Corresponding author. College of Pharmacy, Korea University, 2511 Sejong-ro, Jochiwon-eup, Sejong 339-700, South Korea.
E-mail address: yjbyun1@korea.ac.kr (Y. Byun).
[1] Equal contribution.

http://dx.doi.org/10.1016/j.ejmech.2016.04.033
0223-5234/

[16,17]. The ability to detect overexpression of PSMA has provided novel avenues for the diagnosis and treatment of PCa. Hepsin is also a cell surface serine protease composed of 413 amino acids, with a 255-residue trypsin-like serine protease domain and a 109-residue region that forms a scavenger receptor cysteine-rich (SRCR) domain [18]. Hepsin is overexpressed in up to 90% of prostate tumors, with levels often increased >10 fold in metastatic PCa than in normal prostate or BPH [19,20]. PSMA and hepsin may represent excellent targets for PCa imaging since both have an enzymatic active site in the extracellular region. Imaging probes for the targets do not require penetration of the cell membrane, thus, have less chance of being degraded by metabolic enzymes.

Due to the heterogeneous and multifactorial nature of PCa, the search for novel biomarkers is a key to precise diagnosis and efficient treatment [21]. Recent studies have shifted from the identification of individual biomarkers to the utilization of combinations of known specific markers [22]. A multi-targeting strategy has several advantages over single-targeting. Targeting multiple surface markers simultaneously can improve the sensitivity and specificity of detection through synergistic binding affinities to target proteins. The concept of targeting more than one cell surface protein for imaging purposes has been demonstrated by combining two biomarkers [21–23]. Dual-targeting was found to be more predictive with respect to distinguishing between PCa and BPH than when a single biomarker is targeted [21]. Eder and coworkers developed heterodimer molecules targeting both PSMA and the gastrin-releasing peptide receptor (GRPR), which exhibited high binding affinities to a cell line expressing both GRPR and PSMA [23]. Shallal and coworkers developed heterobivalent agents targeting PSMA and integrin $\alpha_v\beta_3$ [14].

We designed and synthesized a heterobivalent ligand which can bind to PSMA as well as hepsin. We used 2-(4-hydroxybiphenyl-3-yl)-1*H*-indole-5-carboximidamide as a hepsin-binding scaffold while the Lys-urea-Glu moiety served as the PSMA-binding scaffold. The amidine group was reported to interact with Asp189, a key amino acid in the hepsin active site [24]. Lys-urea-Glu moiety was reported to be strong binder to PSMA despite structural modification on the ε-amine of Lys. For *in vitro* cell uptake and *in vivo* imaging studies, we conjugated a PSMA-hepsin ligand with an optical dye SulfoCy7.

2. Results and discussion

2.1. Synthesis of hepsin-targeted analogs

As shown in Scheme 1, hepsin-targeted amidine compounds (**13**–**21**) were synthesized in six steps using commercially available aniline, acetophenone, and arylboronic acids. Preparations of the intermediate imine **2** and the indole-5-carbonitrile **3** were achieved by applying the procedure previously reported by us [25]. Briefly, the N-aryl imine **2** was prepared by reacting 4-aminobenzonitrile with 5′-bromo-2′-hydroxyacetophenone in toluene under piperidine-catalyzed basic condition. The indole-5-carbonitrile **3** was prepared from **2** using $Pd(OAc)_2$ (20 mol%) and Bu_4NBr (2 eq) in DMSO.

The amidine functional group had been reported to interact with the carboxylic acid present in the side chain of Asp 189 in hepsin. Although several methods for directly converting nitrile into an amidine group have been reported [26,27], they were not suitable for the synthesis of a designed PSMA-hepsin conjugate which has labile groups under the reported conditions. Therefore, we utilized an oxadiazole ring as the amidine-protecting group, which can be removed under mild conditions (H_2, Raney-nickel). Reaction of **3** with hydroxylamine in ethanol afforded the oxime analog **4** in 60% yield. Compound **4** was subsequently cyclized to give the oxadiazole **5** using ethyl acetate and ethanol as solvents by modifying a reported procedure [28]. Reaction of **5** with appropriate arylboronic acids under Suzuki Coupling conditions at 100 °C for 4 h, with $Pd(PPh_3)_4$ as a catalyst, Cs_2CO_3 as a base, and DMF/H_2O (5:1) as a solvent, afforded the corresponding biphenyls **6**–**12**. The oxadiazole-containing biphenyls were converted into the final amidines **13**–**21** by applying hydrogenation conditions (H_2, Raney-nickel, 50 psi) for 7 h in a mixture of methanol and acetic acid (7:1) [29]. Deprotection of the oxadiazole ring proceeded in two steps. The O-N bond of the oxadiazole ring is first cleaved, followed by the cleavage of C-N bond. We observed partially-deprotected compounds during HPLC experiments, which have similar retention time to the fully-deprotected amidine compounds **13**–**21**. However, the partially-deprotected compounds were hydrolyzed slowly at room temperature to give the corresponding amidines.

2.2. Synthesis of the heterobivalent ligand

The synthesis of the heterobivalent ligand **30** is outlined in Schemes 2 and 3. The use of protecting group for three hydrophilic functional groups (e.g., amidine, carboxylic acid and amine) was crucial for the preparation of **30**. During the synthesis of **30**, the oxadiazole ring as a protecting group of the amidine was introduced in the first step and removed at the final step because it was highly stable under acidic or basic reaction conditions and also be deprotected by hydrogenation without affecting the other functional groups. Deprotection of the Boc group of compound **9** was achieved using trifluoroacetic acid (TFA) to afford compound **22**. Reaction of **22** with Fmoc-Lys(Boc)-OH under traditional peptide-coupling conditions (HATU in DMF) afforded compound **23** in 56% yield. The Fmoc group of **23** was removed by treatment with 25% piperidine in DMF at room temperature to give compound **24**. The free amine of **24** was conjugated with the tBu-protected Lys-urea-Glu **25**, a known PSMA-binding scaffold [30], to provide compound **26** in 30% yield. Both the tBu and Boc groups of **26** were removed quantitatively using 50% TFA in dichloromethane for 2 h at room temperature to afford compound **27**.

Transformation of the oxadiazole ring of **27** into the amidine group was achieved under hydrogenation conditions (H_2, Raney-nickel, 50 psi) for 4 h in dioxane/water/acetic acid (6:2:1) by modifying a previously published procedure [29].

The hydrogenation reaction of the oxadiazole moiety generated two products, the amidine **28** and the partially-deprotected **29**. The hydrogenation reaction time was critical for the deprotection of the oxadiazole ring. The optimal reaction time was found to be 4 h, with reaction time longer than 4 h generating more by-products through the cleavage of amide bonds. The commercially available SulfoCy7 NHS ester was conjugated to a mixture of **28** and **29** in Tris–HCl buffer (0.1 M, pH 8.5) at room temperature to afford the dye-linked PSMA-hepsin conjugates **30** and **31**. Pure compounds **30** and **31** were obtained by reversed-phase HPLC, applying gradient conditions using 0.5% formic acid in acetonitrile (A) and water (B) as mobile phase (30%–40% A in 20 min; 40%–30% A in 25 min at 3.5 mL/min flow rate) with a retention time of 5.79 min and 6.21 min, respectively. Compound **31** was hydrolyzed slowly at room temperature to give compound **30**.

2.3. Molecular docking study

The reported hepsin X-ray crystal structure (PDB ID: 1O5E) in complex with the amidine-containing ligand (CA-14) was utilized as a template for the docking studies of the synthesized compounds **13**–**21** [24]. The ligand CA-14 presented strong hydrogen-bonding interactions with His57 and Ser195, which were known to be a part of the catalytic triad of hepsin. The positively-charged amidine

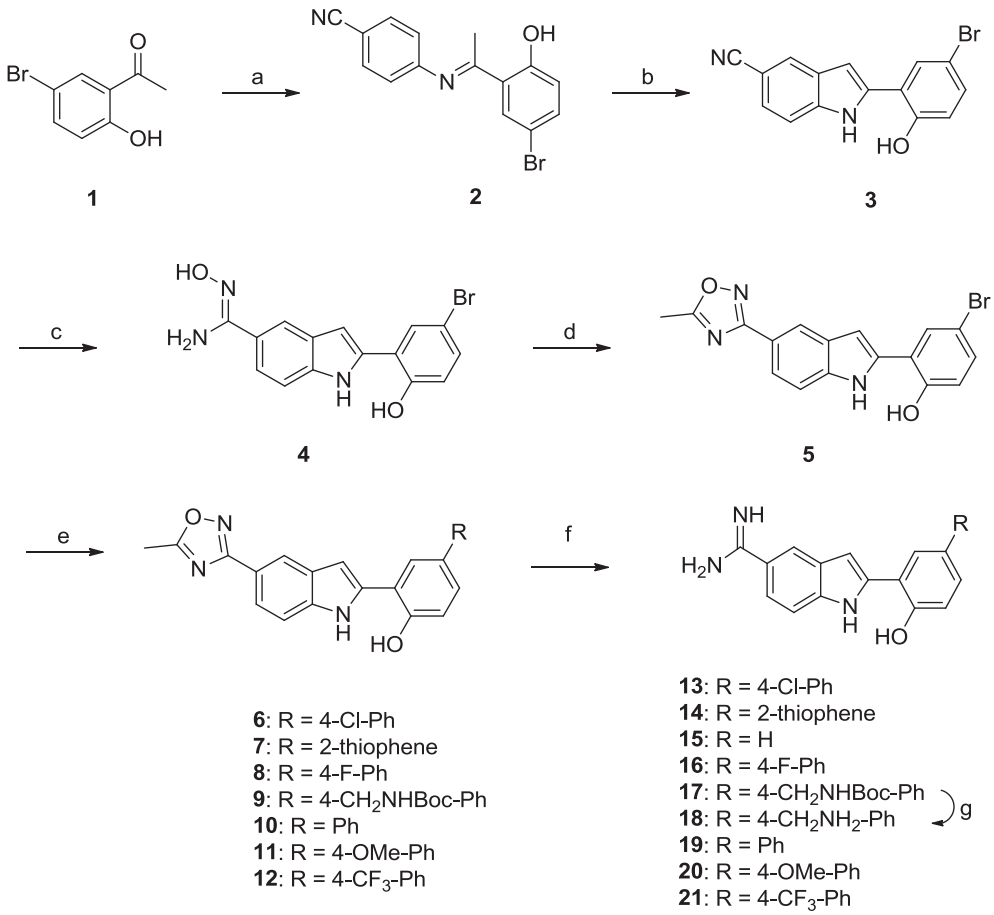

Scheme 1. Synthesis of amidine-containing biphenylindole analogs. **Reagents and conditions**: (a) 4-aminobenzonitrile, piperidine, toluene, 130 °C, 6 h; (b) Bu_4NBr (2 eq), $Pd(OAc)_2$ (20 mol%), DMSO, 110 °C, 12 h; (c) NH_2OH-HCl (10 eq), Na_2CO_3 (5 eq), EtOH, 90 °C, 7 h; (d) NaOEt (2 eq), EtOH/ethylacetate (9/1), 90 °C, 2 h; (e) appropriate boronic acid, Cs_2CO_3, $Pd(PPh_3)_4$, DMF/H_2O (5/1), 100 °C, 4 h; (f) Raney-Ni/H_2, MeOH/AcOH (7/1), 6 h, (g) 50% TFA in CH_2Cl_2, rt, 1 h.

group made strong interactions with the carboxylic acid present in Asp189.

Docking studies of compounds **13**–**21** with hepsin revealed that they were located in the active site similar to the crystal ligand CA-14 [24]. As shown in Fig. 1, the docked pose of compound **19** exhibited an additional interaction with Ser214 as compared with the original ligand.

2.4. In vitro hepsin and PSMA inhibitory activities

For *in vitro* hepsin assay, the known hepsin substrate Boc-Gln-Ala-Arg-AMC was used to determine the hepsin inhibitory activities of the synthesized compounds (**13**–**21** and **30**). The crystal ligand CA-14 (Fig. 1) was synthesized by following a reported procedure [31] and used as a reference for *in vitro* hepsin assay. All of the synthesized compounds (**13**–**21** and **30**) showed inhibitory activity against hepsin similar to CA-14, with IC_{50} values from 5.9 to 70 μM (Table 1). We observed that the amidine moiety is essential for hepsin-binding activity, since none of the compounds (**5**–**12**) with the oxadiazole ring showed hepsin activity. Even the bulky heterobivalent compound **30** exhibited similar hepsin-inhibitory activity (IC_{50} = 2.8 μM) to the monovalent compounds **13**–**21**, indicating that the active site of hepsin tolerates the introduction of bulky groups.

The PSMA inhibitory activities of the PSMA-hepsin conjugates **30** and **31** were determined by measuring the amount of glutamate released from the hydrolysis of *N*-acetyl-L-aspartyl-L-glutamate (NAAG). The IC_{50} values of **30** and **31** were 38 nM and 25 nM, respectively (Fig. 2). Although they were less potent than the urea-based low molecular weight compound **ZJ-43** presumably due to the addition of bulky fluorophore and hepsin binding moieties, **30** and **31** were still sufficiently potent for optical imaging. Previously, the bulky compounds, which consisted of the optical dyes and the PSMA-binding scaffold (Lys-urea-Glu) with IC_{50} values in the double-digit nanomolar concentration range, exhibited strong binding affinity for PSMA-expressing tumors in an *in vivo* study [32].

2.5. In vitro cell uptake study

Cell uptake studies revealed that **30** and **31** specifically bound to PC3/ML-PSMA (PSMA-expressing cell line), PC3/ML-HPN (hepsin-expressing cell line), and PC3/ML-PSMA-HPN (PSMA- and hepsin-expressing cell line) cells (Fig. 3). Both compounds exhibited strong binding affinity for PSMA-expressing cells even at a concentration of 10 nM as compared with PC3/ML cells. The weak binding of the two compounds to PC3/ML-HPN cells might be due to their moderate affinity for hepsin. Both compounds also showed a slightly better uptake at higher concentrations by cells expressing both targets compared with cells expressing PSMA only, indicating synergistic affinity enhancement.

2.6. Preliminary in vivo animal study

We evaluated whether the dual-targeted heterobivalent

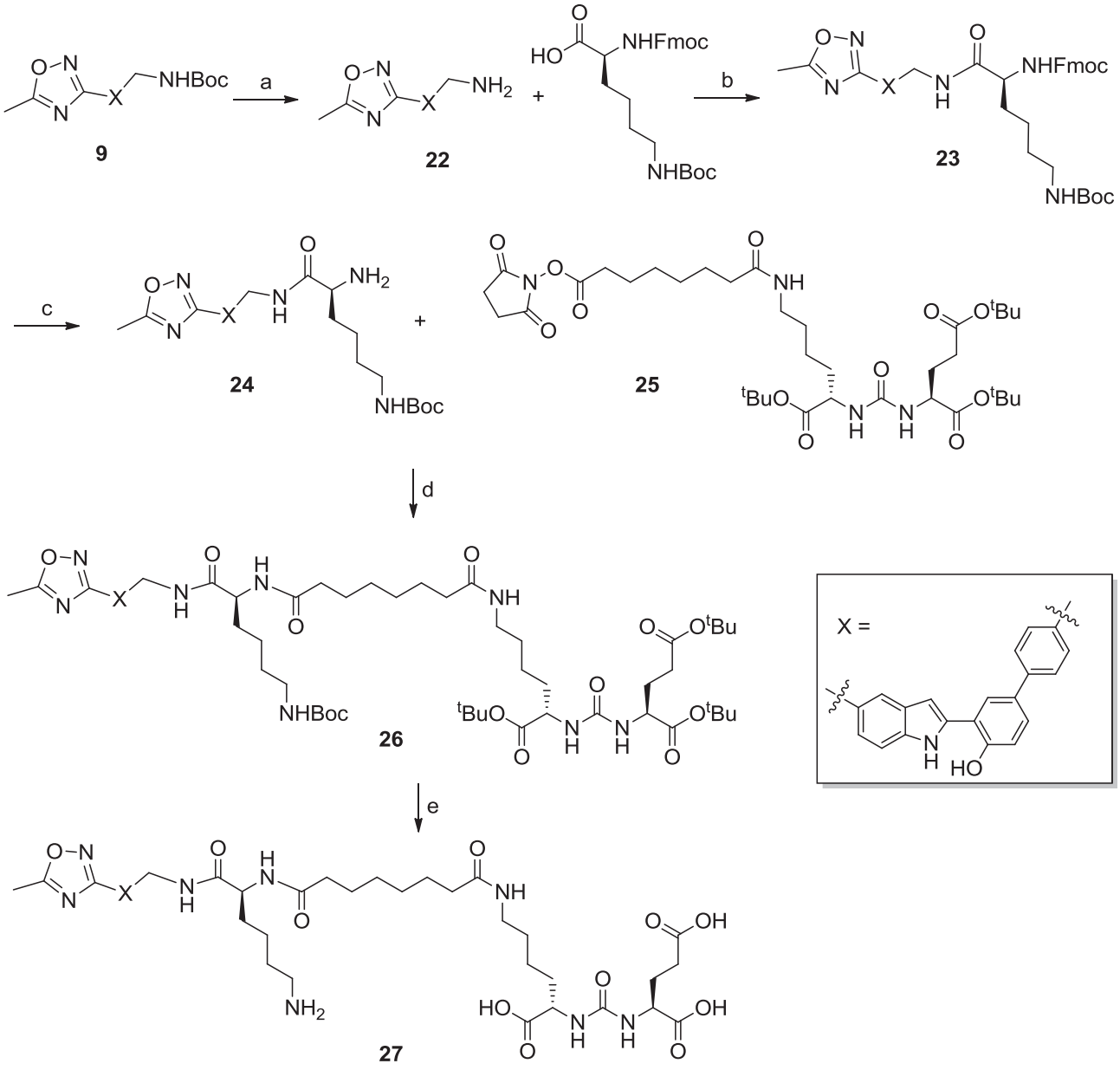

Scheme 2. Synthesis of oxadiazole-protected PSMA-hepsin conjugate **27**. **Reagents and conditions**: (a) 50% TFA in DCM, rt, 1 h; (b) HATU (2 eq), Et_3N (2 eq), DMF, rt, 8 h; (c) 25% piperidine in DMF, rt, 1 h; (d) Et_3N, DMF, rt, 1 h; (e) 50% TFA in DCM, rt, 2 h.

compound **30** is capable of specifically targeting PSMA/hepsin-expressing tumors *in vivo*. We generated a subcutaneous xenograft model of PC3/ML-PSMA (red circle in Fig. 4) and PC3/ML-PSMA-HPN (white circle in Fig. 4), and injected the animal with 1 nmol of **30**. Near infrared (NIR) images were taken at 24 h post-injection, showing that **30** exhibited a higher uptake and retention in the PC3/ML-PSMA-HPN tumor than in the PC3/ML-PSMA tumor.

3. Conclusion

In summary, we designed, synthesized, and evaluated diverse amidine-functionalized analogs as hepsin inhibitors. *In vitro* studies showed that the amidine-containing compounds **13**–**21** exhibited moderate affinity for hepsin. The PSMA-hepsin conjugate **30** was prepared by linking the identified hepsin-binding amidine scaffold with the PSMA-binding Lys-urea-Glu scaffold, followed by conjugation of the optical dye SulfoCy7. Compound **30** exhibited strong binding affinity for PSMA and moderate binding affinity for hepsin. *In vitro* cell uptake and preliminary *in vivo* animal optical imaging studies indicated that **30** have a potential to used as a lead compound in the development of more potent PSMA-hepsin conjugates which may provide a more powerful mechanism for imaging metastatic prostate cancer.

4. Experimental sections

4.1. Chemistry

4.1.1. General

Chemicals and solvents used in the reaction were purchased from Aldrich, Acros, TCI, and Lumiprobe. ^1H NMR and ^{13}C NMR

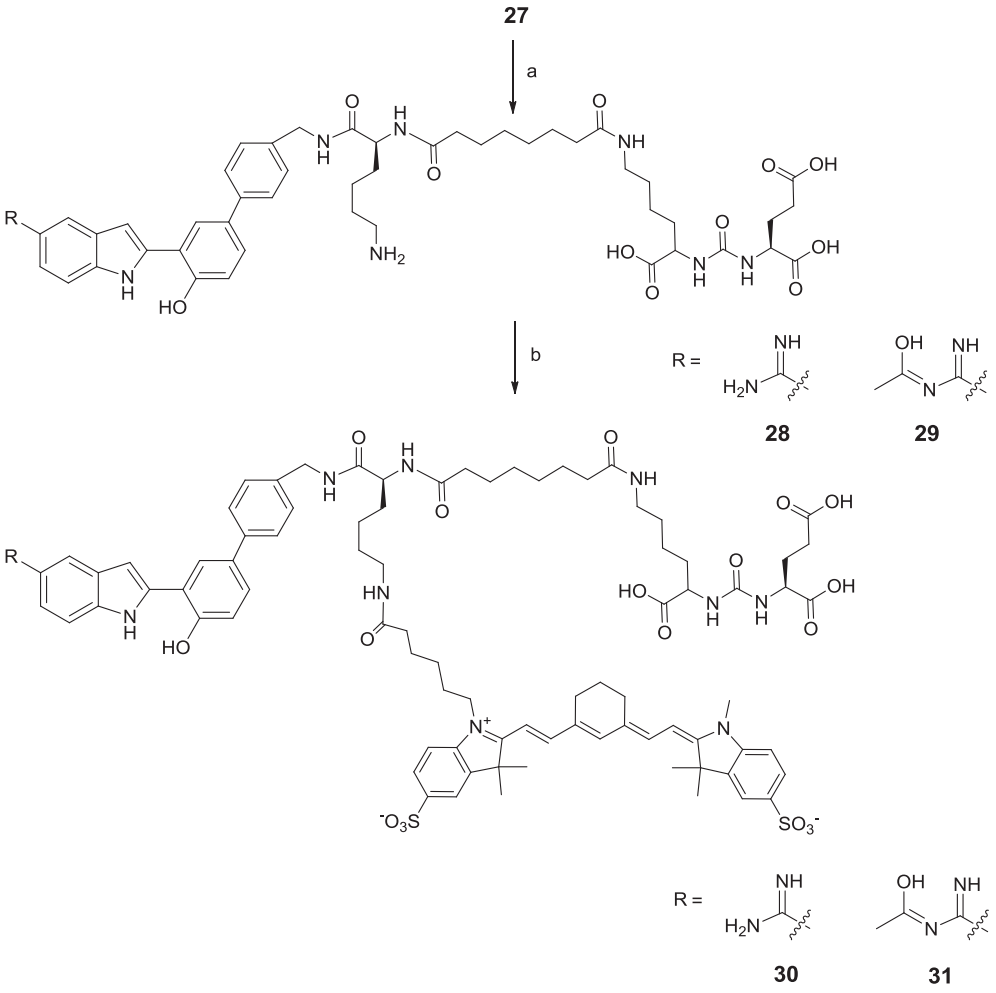

Scheme 3. Synthesis of PSMA-hepsin conjugate **30** labeled with Sulfo-Cy7. **Reagents and conditions**: (a) Raney-Ni/H_2 (50 psi), dioxane/H_2O/AcOH (6:2:1), 4 h; (b) Sulfo-Cy7-NHS ester, Tris–HCl (0.1 M, pH = 8.5), rt, 4 h.

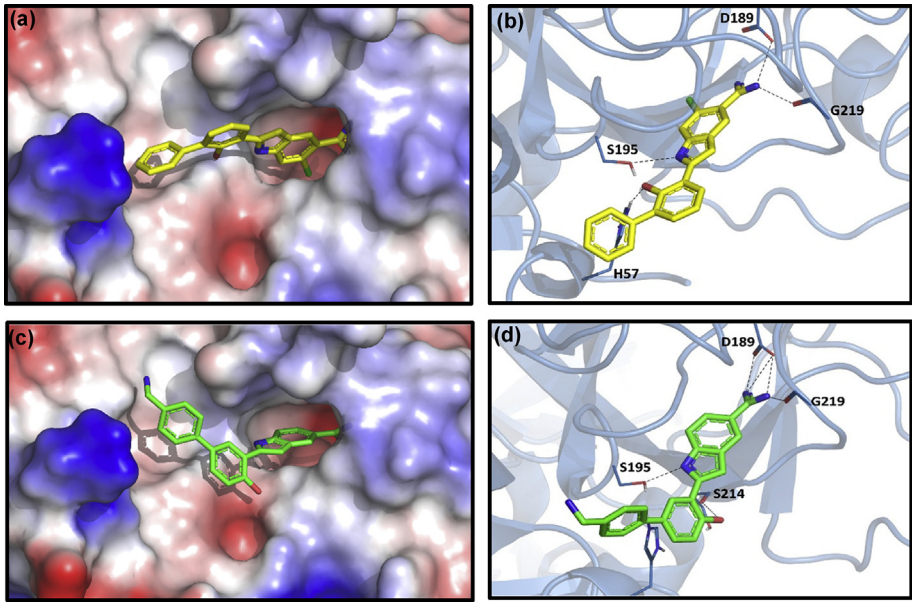

Fig. 1. (a) Binding of **CA-14** (original crystal ligand) to hepsin (b) Expanded view showing hydrogen bonding of **CA-14** to amino acid (c) Binding of **19** to hepsin (d) Expanded view showing hydrogen bonding of **19** to amino acid.

Table 1
IC_{50} value of the prepared amidine-functionalized analogs and the crystal ligand CA-14.

Compound	IC_{50} (μM)
13	23 ± 2.4
14	70 ± 6.4
15	44 ± 3.8
16	5.9 ± 0.5
17	11 ± 1.5
18	9.3 ± 0.4
19	8.9 ± 2.8
20	7.3 ± 0.3
21	14 ± 0.8
30	2.8 ± 0.9
CA-14	2.6 ± 0.1

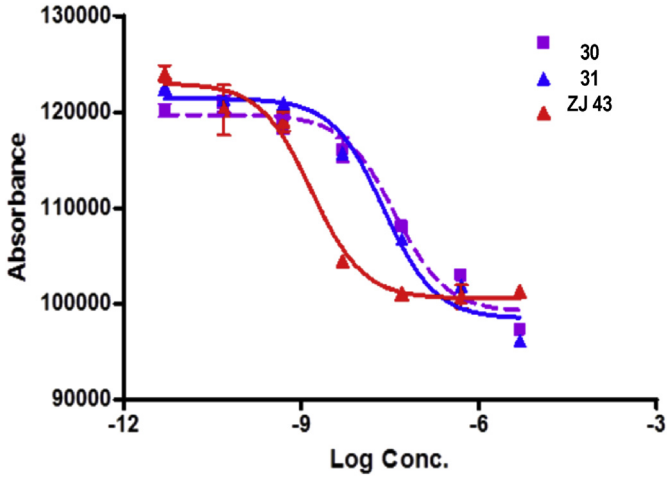

Fig. 2. IC_{50} curves of **30** and **31** to inhibit PSMA.

spectra were carried out on BRUKER Biospin AVANCE 300 MHz and 75 MHz spectrometer, respectively. Chemical shifts were reported as δ values downfield from internal TMS in appropriate organic solvents. Mass spectra were obtained on Agilent 6530 Accurate mass Q-TOF LC/MS spectrometer and Agilent 6460 Triple Quad LC/MS spectrometer. High performance liquid chromatography (HPLC) was carried out on Agilent 1290 Infinity LC using Gemini-NX C18 column (150 mm × 10 mm, 5 μm, 110 Å). Melting points were determined on microscope hot stage apparatus (Linkam THMS 6000). Hydrogenation was carried out using Parr-Hydrogenator (Marathon Electric). Silica gel column chromatography experiments were carried out using Merck Silica Gel F_{254}.

*4.1.2. 4-{(E)-[1-(5-Bromo-2-hydroxyphenyl)ethylidene]amino} benzonitrile (**2**)*

To a solution of 4-aminobenzonitrile (1.00 g, 8.4 mmol) in toluene (10 mL) were added 5′-bromo-2′-hydroxyacetophenone (1.80 g, 8.4 mmol) and piperidine (1 mL). The reaction mixture was stirred at 130 °C for 6 h using Dean–Stark apparatus. The reaction mixture was cooled to room temperature and excess solvent was concentrated to dryness under reduced pressure. The residue was washed with a mixture of hexane and ethylacetate (25 mL × 2) to afford compound **2** as yellow solid. Yield: 56%, R_f: 0.52 (hexane/EA = 9/1), mp: 145–148 °C, ^{1}H NMR (300 MHz, $CDCl_3$): δ 13.70 (s, 1H, NH), 7.78–7.70 (m, 3H, Ar-H), 7.50 (dd, 1H, Ar-H, *J* = 8.7 & 2.4 Hz), 7.02 (d, 2H, Ar-H, *J* = 8.7 Hz), 6.95 (d, 2H, Ar-H, *J* = 9.0 Hz), 2.34 (s, 3H, CH_3), HRMS (ESI): $[M-H]^-$ calcd for C15H11BrN2O: 313.0055, found: 312.9987, ESI-MS/MS: 195.0436 $[M-Br-CN-OH-H]^-$.

*4.1.3. 2-(5-Bromo-2-hydroxyphenyl)-1H-indole-5-carbonitrile (**3**)*

To a solution of compound **2** (0.90 g, 2.9 mmol) in DMSO (10 mL) were added $Pd(OAc)_2$ (65 mg, 0.29 mmol) and Bu_4NBr (1.87 g, 5.8 mmol). The mixture was stirred at 110 °C for 12 h. Upon cooling to room temperature, the reaction mixture was diluted with water (50 mL) and ethyl acetate (50 mL). The combined organic phase was dried over $MgSO_4$, filtered, and concentrated under reduced pressure. The crude residue was purified by silica gel chromatography to afford compound **3** as solid. Yield: 33%, R_f: 0.23 (hexane/EA = 3/1), mp: 103–105 °C, ^{1}H NMR (300 MHz, DMSO-d^6): δ 11.84 (s, 1H, NH), 10.65 (s, 1H, OH), 8.07 (s, 1H, Ar-H), 7.95 (d, 1H, Ar-H, *J* = 8.7 Hz), 7.59 (d, 1H, Ar-H, *J* = 8.7 Hz), 7.45–7.32 (m, 2H, Ar-H), 7.22 (s, 1H, Ar-H), 6.98 (d, 1H, Ar-H, *J* = 8.7 Hz), HRMS (ESI): $[M-H]^-$ calcd for C15H9BrN2O: 310.9898, found: 310.9807, ESI-MS/MS: 231.0576 $[M-Br-H]^-$, 189.0467 $[M-Br-CN-OH-H]^-$.

*4.1.4. (Z)-2-(5-Bromo-2-hydroxyphenyl)-N′-hydroxy-1H-indole-5-carboximidamide (**4**)*

To a solution of compound **3** (0.37 g, 1.2 mmol) in ethanol (20 mL) were added hydroxylamine hydrochloride (0.71 g,

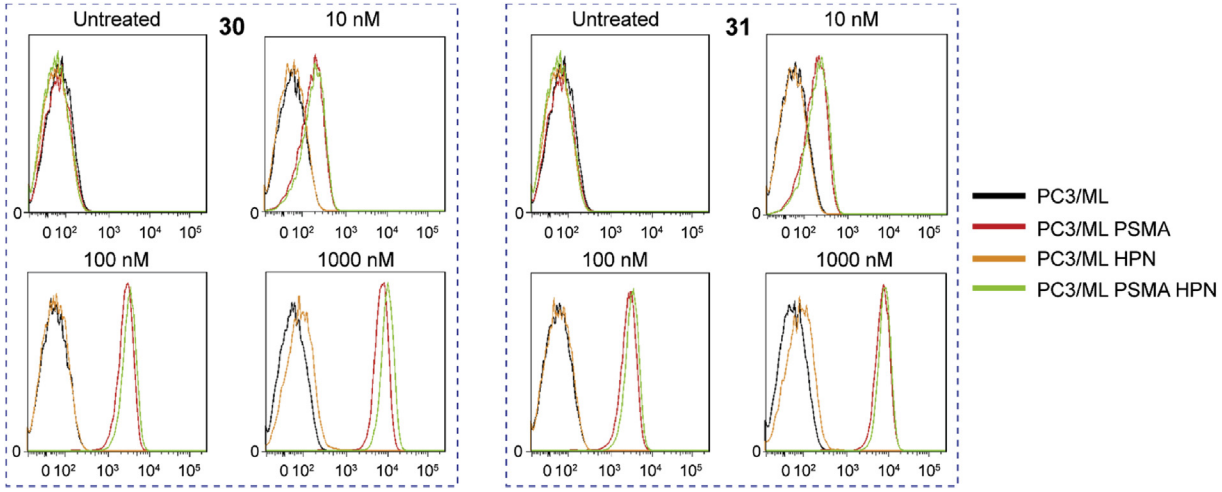

Fig. 3. *In vitro* uptake of **30** and **31** in PC3/ML, PC3/ML-PSMA, PC3/ML-HPN and PC3/ML-PSMA-HPN cell lines.

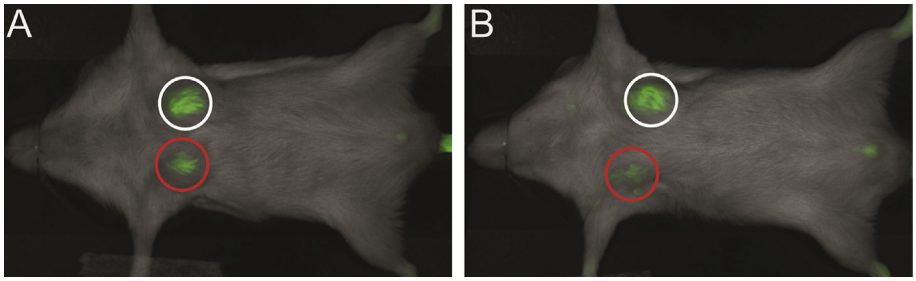

Fig. 4. *In vivo* near infrared imaging of **30** in mice harboring PC3/ML-PSMA (red circles) and PC3/ML-PSMA-HPN (white circles) tumors. Figures A and B represent two independent experiments. (For interpretation of the references to color in this figure legend, the reader is referred to the web version of this article.)

10.2 mmol) and sodium carbonate (0.55 g, 5.1 mmol). The reaction mixture was stirred at 90 °C for 7 h. After the completion of reaction, excess solvent was evaporated to dryness under reduced pressure. The residue was diluted with water (25 mL) and ethyl acetate (25 mL). The combined organic phase was dried over $MgSO_4$, filtered, and concentrated under reduced pressure. The crude residue was purified by silica gel chromatography to afford compound **4** as solid. Yield: 60%, R_f: 0.12 (hexane/EA = 3/1), mp: >400 °C, ^{1}H NMR (300 MHz, DMSO-d^6): δ 11.37 (s, 1H, OH), 9.39 (s, 1H, NH), 8.22 (s, 1H, Ar-H), 7.93 (d, 1H, Ar-H, J = 2.4 Hz), 7.83 (d, 1H, Ar-H, J = 1.2 Hz), 7.49–7.38 (m, 2H, Ar-H), 7.28 (dd, 1H, Ar-H, J = 2.4 & 8.4 Hz), 7.10 (s, 1H, Ar-H), 6.94 (d, 1H, Ar-H, J = 8.7 Hz), 5.71 (s, 2H, NH_2), HRMS (ESI): [M-H]$^-$ calcd for C15H12BrN3O2: 344.0113, found: 344.0068, ESI-MS/MS: 310.9815 [M-NH_2-OH-H]$^-$.

4.1.5. 4-Bromo-2-[5-(5-methyl-1,2,4-oxadiazol-3-yl)-1H-indol-2-yl]phenol (**5**)

To a solution of compound **4** (0.23 g, 0.69 mmol) in ethanol (9 mL) were added sodium ethoxide (90 mg, 1.32 mmol) and ethyl acetate (1 mL). The reaction mixture was stirred at 90 °C for 2 h. After completion of reaction, excess solvent was evaporated to dryness under reduced pressure. The residue was diluted with water (25 mL) and ethyl acetate (25 mL). The organic phase was dried over $MgSO_4$, filtered, and concentrated under reduced pressure. The crude residue was purified by silica gel chromatography to afford compound **5** as solid. Yield: 42%, R_f: 0.25 (hexane/EA = 3/1), mp: 236–238 °C, ^{1}H NMR (300 MHz, DMSO-d^6): δ 11.61 (s, 1H, NH), 10.59 (s, 1H, OH), 8.22 (s, 1H, Ar-H), 7.95 (d, 1H, Ar-H, J = 2.4 Hz), 7.74 (dd, 1H, Ar-H, J = 8.4 & 1.5 Hz), 7.58 (d, 1H, Ar-H, J = 8.4 Hz), 7.33 (dd, 1H, Ar-H, J = 2.4 & 8.7 Hz), 7.21 (s, 1H, Ar-H), 6.97 (d, 1H, Ar-H, J = 8.7 Hz), 2.66 (s, 3H, CH_3), 13C NMR (75 MHz, DMSO-d_6): δ 117.17, 154.31, 138.36, 135.51, 131.38, 129.78, 128.68, 121.10, 120.72, 120.28, 119.00, 117.82, 112.54, 111.16, 103.52, 12.49 (CH_3), HRMS (ESI): [M-H]$^-$ calcd for C17H12BrN3O2: 368.0113, found: 368.0025, ESI-MS/MS: 327.1152 [M-Ac-OH-H]$^-$.

4.1.6. 4′-Chloro-3-[5-(5-methyl-1,2,4-oxadiazol-3-yl)-1H-indol-2-yl][1,1′-biphenyl]-4-ol (**6**)

To a solution of compound **5** (100 mg, 0.27 mmol) in DMF (5 mL) were added 4-chlorophenyl boronic acid (42 mg, 0.27 mmol), cesium carbonate (182 mg, 0.55 mmol in 1 mL water) and $Pd(PPh_3)_4$ (16 mg, 0.014 mmol). The reaction mixture was stirred at 100 °C for 4 h. Upon cooling to room temperature, the reaction mixture was diluted with water (30 mL) and ethyl acetate (15 mL). The solution pH was adjusted to 7 by using 1 N HCl. The organic phase was dried over $MgSO_4$, filtered, and concentrated under reduced pressure. The residue was purified by silica gel chromatography to afford compound **6**. Yield: 30%, R_f: 0.25 (hexane/EA = 3/1), LRMS (ESI): [M-H]$^-$ calcd for C23H16ClN3O2: 400.1, found: 400.1, ESI-MS/MS: 290.1 [M-Ph-Cl-H]$^-$.

4.1.7. 2-[5-(5-Methyl-1,2,4-oxadiazol-3-yl)-1H-indol-2-yl]-4-(thiophen-2-yl)phenol (**7**)

In the same method as **6**, 2-thienylboronic acid was used instead of 4-chlorophenylboronic acid. Yield: 33%, R_f: 0.25 (hexane/EA = 3/1), LRMS (ESI): [M-H]$^-$ calcd for $C_{21}H_{15}N_3O_2S$: 372.1, found: 372.0, ESI-MS/MS: 315.0 [M-Ac-NH_2]$^-$.

4.1.8. 4′-Fluoro-3-[5-(5-methyl-1,2,4-oxadiazol-3-yl)-1H-indol-2-yl][1,1′-biphenyl]-4-ol (**8**)

In the same method as **6**, 4-fluorophenyboronic acid was used instead of 4-chlorophenylboronic acid. Yield: 34%, R_f: 0.27 (hexane/EA = 3/1), LRMS (ESI): [M-H]$^-$ calcd for $C_{23}H_{16}FN_3O_2$: 384.1, found: 384.1, ESI-MS/MS: 290.1 [M-Ph-F-H]$^-$.

4.1.9. tert-Butyl({4′-hydroxy-3′-[5-(5-methyl-1,2,4-oxadiazol-3-yl)-1H-indol-2-yl][1,1′-biphenyl]-4-yl}methyl)carbamate (**9**)

To a solution of 4-aminomethylphenylboronic acid (2.65 mmol) in THF (10 mL) were added di-*tert*-butyl dicarbonate (3.97 mmol) and triethylamine (1 mL). The mixture was stirred at room temperature for 1 h. After completion of the reaction, excess solvent was evaporated to dryness under reduced pressure. The residue was diluted with water (30 mL) and ethyl acetate (15 mL). The organic phase was separated, dried over $MgSO_4$, filtered, and concentrated under reduced pressure. The NHBoc-protected boronic acid was then used for Suzuki coupling as described in compound **6** to afford compound **9**. Yield: 32%, R_f: 0.31 (hexane/EA = 3/2), mp: 147–148 °C, ^{1}H NMR (300 MHz, DMSO-d^6): δ 11.63 (br s, 1H, NH), 10.39 (br s, 1H, OH), 8.22 (s, 1H, Ar-H), 8.07 (d, 1H, Ar-H, J = 2.4 Hz), 7.76–7.64 (m, 3H, Ar-H), 7.59 (d, 1H, Ar-H, J = 8.4 Hz), 7.51–7.42 (m, 2H, Ar-H), 7.32 (d, 2H, Ar-H, J = 8.1 Hz), 7.23 (s, 1H, Ar-H), 7.10 (d, 1H, Ar-H, J = 8.4 Hz), 4.17 (d, 2H, J = 6.0 Hz, CH_2), 2.66 (s, 3H, OCH_3), 1.41 (s, 9H, (CH3)3), HRMS (ESI): [M-H]$^-$ calcd for C29H28N4O4: 495.2111, found: 495.1981, ESI-MS/MS: 439.1448 [M-Ac-NH_2]$^-$, 395.1550 [M-Boc-H]$^-$.

4.1.10. 3-[5-(5-Methyl-1,2,4-oxadiazol-3-yl)-1H-indol-2-yl][1,1′-biphenyl]-4-ol (**10**)

In the same method as **6**, phenylboronic acid was used instead of 4-chlorophenylboronic acid. Yield: 37%, R_f: 0.23 (hexane/EA = 3/1), LRMS (ESI): [M-H]$^-$ calcd for C23H17N3O2: 366.1, found: 366.1.

4.1.11. 4′-Methoxy-3-[5-(5-methyl-1,2,4-oxadiazol-3-yl)-1H-indol-2-yl][1,1′-biphenyl]-4-ol (**11**)

In the same method as **6**, 4-methoxyphenyboronic acid was used instead of 4-chlorophenylboronic acid. Yield: 36%, R_f: 0.27 (hexane/EA = 3/1), LRMS (ESI): [M-H]$^-$ calcd for C24H19N3O3: 396.1, found: 396.2.

*4.1.12. 3-[5-(5-Methyl-1,2,4-oxadiazol-3-yl)-1H-indol-2-yl]-4′-(trifluoromethyl)[1,1′-biphenyl]-4-ol (**12**)*

In the same method as **6**, 4-trifluoromethyphenyboronic acid was used instead of 4-chlorophenylboronic acid. Yield: 39%, R_f: 0.26 (hexane/EA = 3/1), LRMS (ESI): $[M-H]^-$ calcd for C24H16F3N3O2: 434.1, found: 434.1.

*4.1.13. 2-(4′-Chloro-4-hydroxy[1,1′-biphenyl]-3-yl)-1H-indole-5-carboximidamide (**13**)*

To a solution of compound **5** in a mixture of MeOH and AcOH (10 mL, 7:1) was added a catalytic amount of Raney-nickel. The reaction mixture was shaken under 50 psi of H_2 for 7 h. The mixture was filtered through Celite and the filtrate was concentrated to dryness under reduced pressure. The residue was purified by reversed-phase HPLC to afford compound **13**. HPLC: 80/20 water/acetonitrile (0.1% formic acid), flow rate 2 mL/min, R_t = 9.15 min, Yield: 22%, mp: 126–128 °C, ^{1}H NMR (300 MHz, CD_3OD): δ 8.58 (s, 2H, NH_2), 8.11 (s, 1H, Ar-H), 8.01 (d, 1H, Ar-H, *J* = 2.4 Hz), 7.67–7.57 (m, 3H, Ar-H), 7.54–7.45 (m, 1H, Ar-H), 7.45–7.25 (m, 4H, Ar-H), 6.99 (d, 1H, Ar-H, *J* = 8.4 Hz), 13C NMR (75 MHz, CD_3OD): 168.92, 168.03, 158.67, 140.43, 139.78, 139.22, 131.78, 129.40, 128.60, 128.37, 127.37, 127.30, 125.45, 120.19, 119.33, 118.53, 117.93, 111.33. HRMS (ESI): $[M+H]^+$ calcd for C21H16ClN3O: 362.0982, found: 362.1053, ESI-MS/MS: 345.0763 $[M-NH_3+H]^+$, 320.0793 $[M-NH_3-CN+H]^+$.

*4.1.14. 2-[2-Hydroxy-5-(thiophen-2-yl)phenyl]-1H-indole-5-carboximidamide (**14**)*

In the same method as **13**, compound **14** was prepared from **7**. HPLC: 70/30 water/acetonitrile (0.1% formic acid), flow rate 2 mL/min; R_t = 8.71 min, Yield: 37%, mp: 240–243 °C, ^{1}H NMR (300 MHz, CD_3OD): δ 8.58 (s, 4H), 8.14 (s, 1H, Ar-H), 8.04 (d, 1H, Ar-H, *J* = 2.1 Hz), 7.66 (d, 1H, Ar-H, *J* = 8.4 Hz), 7.56–7.50 (m, 1H, Ar-H), 7.47 (dd, 1H, Ar-H, *J* = 8.4 & 2.4 Hz), 7.37–7.28 (m, 2H, Ar-H), 7.19 (s, 1H, Ar-H), 7.13–7.04 (m, 1H, Ar-H), 7.00 (d, 1H, Ar-H, *J* = 8.4 Hz), 13C NMR (75 MHz, CD_3OD): 168.99, 167.98, 154.86, 144.01, 139.61, 138.61, 128.45, 127.59, 126.45, 124.78, 123.34, 121.80, 120.54, 119.79, 118.51, 118.22, 116.90, 111.54, HRMS (ESI): $[M+H]^+$ calcd for C19H15N3OS: 334.0936, found: 334.1013, ESI-MS/MS: 317.0727 $[M-NH_3+H]^+$, 292.0788 $[M-NH_3-CN+H]^+$.

*4.1.15. 2-(4-Hydroxy[1,1′-biphenyl]-3-yl)-1H-indole-5-carboximidamide (**15**)*

In the same method as **13**, compound **15** was prepared from **5**. HPLC: acetonitrile (A)/water (B) (0.1% formic acid), the gradient consisted of 10% A to 90% A over 30 min at 2 mL/min flow rate. R_t = 9.78 min. Yield: 46%, mp: 181–183 °C, ^{1}H NMR (300 MHz, CD_3CN/D_2O): δ 8.48 (s, 1H, NH), 8.18 (s, 1H, Ar-H), 7.88 (d, 1H, Ar-H, *J* = 7.8 Hz), 7.73 (d, 1H, Ar-H, *J* = 8.7 Hz), 7.65–7.56 (m, 1H, Ar-H), 7.39–7.29 (m, 1H, Ar-H), 7.12 (s, 1H, Ar-H), 7.15–6.95 (m, 2H, Ar-H), 13C NMR (75 MHz, CD_3CN/D_2O): 170.52, 167.61, 154.28, 139.82, 139.29, 130.23, 128.61, 121.63, 121.43, 121.04, 120.88, 118.22, 117.18, 112.62, 101.09, HRMS (ESI): $[M+H]^+$ calcd for C15H13N3O: 252.1059, found: 252.1134, ESI-MS/MS: 235.0863 $[M-NH_3+H]^+$, 210.0902 $[M-NH_3-CN+H]^+$.

*4.1.16. 2-(4′-Fluoro-4-hydroxy[1,1′-biphenyl]-3-yl)-1H-indole-5-carboximidamide (**16**)*

In the same method as **13**, compound **16** was prepared from **8**. HPLC: acetonitrile (A)/water (B) (0.1% formic acid), the gradient consisted of 40% A to 50% A over 30 min at 2 mL/min flow rate. R_t = 9.78 min. Yield: 30%, mp: 165–168 °C, ^{1}H NMR (300 MHz, CD_3OD): δ 8.14 (s, 1H, Ar-H), 8.03 (d, 1H, Ar-H, *J* = 2.1 Hz), 7.68–7.60 (m, 3H, Ar-H), 7.57–7.45 (m, 2H, Ar-H), 7.37 (d, 1H, Ar-H, *J* = 8.1 Hz), 7.22 (s, 1H, Ar-H), 7.06 (d, 1H, Ar-H, *J* = 8.4 Hz), 13C NMR (75 MHz, CD_3OD): 167.95, 163.79, 154.07, 139.67, 138.65, 137.00, 132.10, 128.56, 128.49, 128.00, 127.90, 127.33, 125.88, 120.60, 119.83, 118.40, 118.19, 116.55, 115.17, 114.89, 111.53, 101.26, HRMS (ESI) MS: $[M+H]^+$ calcd for C21H16FN3O: 346.1277, found: 346.1361, ESI-MS/MS: 330.2389 $[M-NH_3+H]^+$, 305.2931 $[M-NH_3-CN+H]^+$.

*4.1.17. tert-Butyl{[3′-(5-carbamimidoyl-1H-indol-2-yl)-4′-hydroxy[1,1′-biphenyl]-4-yl] methyl} carbamate (**17**)*

In the same method as **13**, compound **17** was prepared from **9**. HPLC: 70/30 water/acetonitrile (0.1% formic acid), flow rate 2 mL/min, R_t = 5.94 min, Yield: 40%, mp: 196–199 °C, ^{1}H NMR (300 MHz, CD_3OD): δ 8.14 (s, 1H, Ar-H), 8.00 (d, 1H, Ar-H, *J* = 2.1 Hz), 7.71–7.63 (m, 3H, Ar-H), 7.57–7.52 (m, 1H, Ar-H), 7.45 (dd, 1H, Ar-H, *J* = 8.4 & 2.1 Hz), 7.24–7.14 (m, 3H, Ar-H), 7.07 (d, 1H, Ar-H, *J* = 8.4 Hz), 4.23 (s, 2H, CH_2), 1.49 (s, 9H, (CH3)3), 13C NMR (75 MHz, CD_3OD): 167.97, 157.22, 154.03, 139.68, 139.33, 138.77, 138.12, 132.80, 128.59, 128.51, 127.34, 127.25, 126.19, 125.83, 120.58, 119.79, 118.34, 118.16, 116.51, 111.52, 101.20, 78.82, 43.35 (CH_2), 27.38 (CH3)3, HRMS (ESI) MS: $[M+H]^+$ calcd for C27H28N4O3: 457.2162, found: 457.2225, ESI-MS/MS: 357.3035 $[M-Boc+H]^+$ 341.2742 $[M-Boc-NH_2+H]^+$, 324.2468 $[M-Boc-NH_2-NH_3+H]^+$, 299.2524 $[M-Boc-NH_2-NH_3-CN+H]^+$.

*4.1.18. 2-[4′-(Aminomethyl)-4-hydroxy[1,1′-biphenyl]-3-yl]-1H-indole-5-carboximidamide (**18**)*

Compound **17** (10 mg, 0.02 mmol) was dissolved in a mixture of TFA and dichloromethane (2 mL, 1:1). The reaction mixture was stirred at room temperature for 1 h. The mixture was concentrated to dryness under reduced pressure. The residue was dissolved in a mixture of water and acetonitrile and purified by reversed-phase HPLC to give compound **18**. HPLC: 70/30 water/acetonitrile (0.1% formic acid), flow rate 2 mL/min, R_t = 2.56 min. Yield: 72%, mp: 126–129 °C, ^{1}H NMR (300 MHz, CD_3CN/D_2O): δ 8.49 (d, 2H, Ar-H, *J* = 7.2 Hz), 8.14 (d, 1H, Ar-H, *J* = 8.1 Hz), 8.06 (d, 1H, Ar-H, *J* = 8.7 Hz), 8.01–7.87 (m, 4H, Ar-H), 7.61 (s, 1H, Ar-H), 7.53 (d, 1H, Ar-H, *J* = 8.4 Hz), 4.54 (s, 2H, CH_2), 13C NMR (75 MHz, CD_3CN/D_2O): 167.57, 161.90, 154.34, 141.20, 139.86, 132.61, 131.91, 130.12, 128.62, 127.50, 126.89, 121.53, 121.05, 117.79, 112.66, 101.63, 43.15 (CH_2), HRMS (ESI) MS: $[M+H]^+$ calcd for C22H20N4O: 357.1637, found: 357.1711, ESI-MS/MS: 340.2968 $[M-NH_3+H]^-$, 323.2406 $[M-NH_3-NH_3+H]^+$, 315.2702 $[M-NH_3-CN+H]^+$.

*4.1.19. 2-(4-Hydroxy[1,1′-biphenyl]-3-yl)-1H-indole-5-carboximidamide (**19**)*

In the same method as **13**, compound **19** was prepared from **10**. HPLC: 72/28 water/acetonitrile (0.1% formic acid), flow rate 2 mL/min, R_t = 8.62 min, Yield: 42%, mp: 220–223 °C, ^{1}H NMR (300 MHz, CD_3CN/D_2O): δ 8.76 (s, 1H, NH), 8.48 (s, 1H, Ar-H), 8.43 (s, 1H, Ar-H), 8.10–7.97 (m, 3H, Ar-H), 7.96–7.80 (m, 5H, Ar-H), 7.78–7.70 (m, 1H, Ar-H), 7.57 (s, 1H, Ar-H), 7.49 (d, 1H, Ar-H, *J* = 8.4 Hz), ^{13}C NMR (75 MHz, CD_3CN/D_2O): 153.94, 140.49, 139.78, 138.84, 134.31, 133.52, 131.24, 129.45, 128.29, 127.57, 127.36, 126.91, 126.77, 121.41, 120.94, 117.67, 112.98, HRMS (ESI) MS: $[M+H]^+$ calcd for $C_{21}H_{17}N_3O$: 328.1372, found: 328.1435, ESI-MS/MS: 311.2381 $[M-NH_3+H]^+$, 286.2379 $[M-NH_3-CN+H]^+$.

*4.1.20. 2-(4-Hydroxy-4′-methoxy[1,1′-biphenyl]-3-yl)-1H-indole-5-carboximidamide (**20**)*

In the same method as **13**, compound **20** was prepared from **11**. HPLC: 75/25 water/acetonitrile(0.1% formic acid), flow rate 2 mL/min, R_t = 12.98 min, Yield: 33%, mp: 132–135 °C, ^{1}H NMR (300 MHz, CD_3CN/D_2O): δ 8.48 (s, 1H, NH), 8.19 (s, 1H, Ar-H), 8.08 (d, 1H, Ar-H, *J* = 2.4 Hz), 7.80–7.68 (m, 3H, Ar-H), 7.65–7.52 (m, 2H, Ar-H), 7.29 (s, 1H, Ar-H), 7.22–7.10 (m, 3H, Ar-H), 6.92–6.82 (m, 1H, Ar-H), 3.85 (s, 3H, OCH_3), 13C NMR (75 MHz, CD_3CN/D_2O): 172.68, 169.92, 161.54, 156.06, 142.12, 135.61, 135.43, 130.91, 130.83, 130.41,

128.58, 123.75, 123.23, 120.0, 118.67, 117.63, 117.11, 114.88, 103.69, 57.94 ($O\underline{C}H_3$), HRMS (ESI): $[M+H]^+$ calcd for $C_{22}H_{19}N_3O_2$: 358.1477, found: 358.1564, ESI-MS/MS: 341.2541 $[M-NH_3+H]^+$, 326.2285 $[M-NH_3-OH+H]^+$, 316.2550 $[M-NH_3-CN+H]^+$, 298.2271 $[M-NH_3-CN-OH+H]^+$.

*4.1.21. 2-[4-Hydroxy-4′-(trifluoromethyl)[1,1′-biphenyl]-3-yl]-1H-indole-5-carboximidamide (**21**)*

In the same method as **13**, compound **21** was prepared from **12**. HPLC: 68/32 water/acetonitrile(0.1% formic acid), flow rate 2 mL/min, Rt = 9.92 min. Yield: 28%, mp: 191–193 °C, ^{1}H NMR (300 MHz, CD_3CN/D_2O): δ 8.53 (s, 2H, Ar-H), 8.29 (d, 2H, Ar-H, J = 7.5 Hz), 8.19 (d, 2H, Ar-H, J = 7.8 Hz), 8.12–7.90 (m, 4H, Ar-H), 7.63 (s, 1H, Ar-H), 7.56 (d, 1H, Ar-H, J = 8.4 Hz), ^{13}C NMR (75 MHz, CD_3CN/D_2O): 167.59, 154.84, 144.48, 139.88, 131.86, 128.79, 127.48, 127.22, 126.28, 121.56, 121.10, 117.88, 112.68, 101.78, LRMS (ESI): $[M+H]^+$ calcd for $C_{22}H_{16}F_3N_3O$: 396.1245, found: 396.1272, ESI-MS/MS: 379.2376 $[M-NH_3+H]^+$, 354.2366 $[M-NH_3-CN+H]^+$.

*4.1.22. 4′-(Aminomethyl)-3-[5-(5-methyl-1,2,4-oxadiazol-3-yl)-1H-indol-2-yl][1,1′-biphenyl]-4-ol (**22**)*

Compound **9** (300 mg, 0.60 mmol) was dissolved in a mixture of TFA and dichloromethane (5 mL, 1:1). The reaction mixture was stirred at room temperature for 1 h. The mixture was concentrated under reduced pressure and used for next step without further purification. LRMS (ESI): $[M-H]^-$ calcd for C24H20N4O2: 395.1, found: 395.0.

*4.1.23. (9H-Fluoren-9-yl)methyl N-{1-[({4′-hydroxy-3′-[5-(5-methyl-1,2,4-oxadiazol-3-yl)-1H-indol-2-yl]-[1,1′-biphenyl]-4-yl}methyl)carbamoyl]-5-{[(propan-2-yloxy)carbonyl]amino} pentyl} carbamate (**23**)*

To a solution of compound **22** (100 mg, 0.26 mmol) in DMF (15 mL) were added HATU (192 mg, 0.50 mmol), Fmoc-Lys(Boc)-OH (140 mg, 0.3 mmol), and triethylamine (70 μL, 0.50 mmol). The reaction mixture was stirred at room temperature for 8 h. The reaction mixture was diluted with water (30 mL) and ethyl acetate (15 mL). The solution pH was adjusted to 7 by using 1 N HCl. The organic phase was dried over $MgSO_4$, filtered and concentrated under reduced pressure. The crude residue was purified by silica gel chromatography to afford compound **23**. Yield: 56%, R_f: 0.41 (hexane/EA = 3/2), ^{1}H NMR (300 MHz, DMSO-d^6): δ 11.84 (s, 1H, NH), 8.52–8.45 (m, 1H, Ar-H), 8.26 (s, 1H, Ar-H), 8.09 (d, 1H, Ar-H, J = 12 Hz), 7.96 (s, 4H, Ar-H), 7.87 (d, 3H, Ar-H, J = 7.5 Hz), 7.81–7.62 (m, 6H, Ar-H), 7.54 (d, 2H, Ar-H, J = 8.4 Hz), 7.43–7.20 (m, 9H, Ar-H), 7.06 (s, 1H, Ar-H), 6.82–6.74 (m, 1H, Ar-H), 4.46–4.32 (m, 4H), 4.30–4.20 (m, 4H), 4.08–3.95 (m, 2H), 2.69 (s, 1H), 2.59 (s, 3H, $C\underline{H}_3$), 1.35 (s, 9H, $(C\underline{H}_3)_3$).

*4.1.24. tert-Butyl N-{5-amino-5-[({4′-hydroxy-3′-[5-(5-methyl-1,2,4-oxadiazol-3-yl)-1H-indol-2-yl][1,1′-biphenyl]-4-yl}tmethyl) carbamoyl]pentyl}carbamate (**24**)*

Compound **23** (50 mg, 0.06 mmol) was dissolved in 25% piperidine in DMF (5 mL) and stirred at room temperature for 1 h. The mixture was concentrated to dryness under reduced pressure and used for next step without purification. LRMS (ESI): $[M+Na]^+$ calcd for C35H40N6O5: 647.3, found: 647.4.

*4.1.25. 1,5-Di-tert-butyl 2-({[1-(tert-butoxy)-6-{7-[(5-{[(tert-butoxy)carbonyl]amino}-1-[({4′-hydroxy-3′-[5-(5-methyl-1,2,4-oxadiazol-3-yl)-1H-indol-2-yl][1,1′-biphenyl]-4-yl}methyl) carbamoyl]pentyl)carbamoyl]heptanamido}-1-oxohexan-2-yl] carbamoyl}amino)pentanedioate (**26**)*

To a solution of compound **24** (50 mg, 0.08 mmol) in DMF (10 mL) were added trimethylamine (0.05 mL) and compound **25** (59 mg, 0.08 mmol) which was prepared by applying a reported procedure [30]. The mixture was stirred at room temperature for 1 h. The reaction mixture was diluted with water (30 mL) and ethyl acetate (15 mL). The solution pH was adjusted to 7 by using 1 N HCl. The combined organic phase was dried over $MgSO_4$, filtered and concentrated under reduced pressure. The crude residue was purified by silica gel chromatography to afford compound **26**. Yield: 30%, R_f: 0.38 (ethylacetate/methanol = 10/1), ^{1}H NMR (300 MHz, CD_3OD): δ 8.28 (s, 1H), 8.05–7.92 (m, 1H, Ar-H), 7.88–7.54 (m, 1H, Ar-H), 7.52–7.60 (m, 3H, Ar-H), 7.59–7.50 (m, 2H, Ar-H), 7.48–7.32 (m, 3H, Ar-H), 7.17–7.10 (m, 2H, Ar-H), 6.90–6.70 (m, 1H), 6.52–6.64 (m, 1H), 6.42–6.30 (m, 2H), 4.51–4.41 (m, 3H), 4.39–4.32 (m, 2H), 4.29 (s, 1H), 4.23–4.09 (m, 7H), 3.22–3.10 (m, 6H), 3.08–2.98 (m, 5H), 2.71–2.62 (m, 4H), 2.45–2.23 (m, 11H), 2.20–2.10 (m, 8H), 2.08–1.97 (m, 4H), 1.58–1.70 (m, 18H), 1.56–1.10 (m, 36H).

*4.1.26. 2-[({5-[7-({5-Amino-1-[({4′-hydroxy-3′-[5-(5-methyl-1,2,4-oxadiazol-3-yl)-1H-indol-2-yl][1,1′-biphenyl]-4-yl}methyl) carbamoyl]pentyl}carbamoyl)heptanamido]-1-carboxypentyl} carbamoyl)amino]pentanedioic acid (**27**)*

Compound **26** (20 mg, 0.02 mmol) was dissolved in a mixture of TFA and dichloromethane (5 mL, 1:1) and stirred at room temperature for 2 h. The mixture was concentrated under reduced pressure. The residue was purified by reversed-phase HPLC to afford compound **27**. HPLC: 72/28 water/acetonitrile (0.1% formic acid), flow rate 2 mL/min; R_t = 11.68 min. Yield: 25%, mp: 205–207 °C, ^{1}H NMR (300 MHz, CD_3CN/D_2O): δ 8.16 (s, 1H, Ar-H), 7.94 (s, 1H, Ar-H), 7.60 (d, 1H, Ar-H, J = 8.7 Hz), 7.53 (t, 3H, Ar-H, J = 7.5 Hz), 7.40 (d, 1H, Ar-H, J = 8.4 Hz), 7.25 (d, 2H, Ar-H, J = 9.0 Hz), 7.05 (m, 2H, Ar-H), 4.29 (s, 2H), 3.98 (m, 2H), 2.96 (t, 2H, J = 6.8 Hz), 2.81 (t, 2H, J = 7.7 Hz), 2.53 (s, 3H), 2.29 (t, 2H, J = 7.5 Hz), 2.15 (t, 2H, J = 7.4 Hz), 1.98 (t, 2H, J = 7.2 Hz), 1.58–1.82 (m, 24H), ^{13}C NMR (75 MHz, CD_3CN/D_2O): 180.44, 178.72, 178.33, 176.17, 171.72, 156.20, 141.78, 140.69, 140.03, 139.85, 135.31, 131.01, 130.59, 130.35, 129.34, 128.79, 123.13, 120.17, 119.94, 114.83, 56.44, 56.21, 56.05, 45.07, 41.88, 41.57, 38.45, 38.21, 34.19, 33.42, 33.18, 30.98, 30.86, 30.80, 30.19, 28.98, 28.04, 27.98, 25.25, 25.07, 14.37, HRMS (ESI): $[M+H]^+$ calcd for C50H63N9O12: 982.4596, found: 982.4715, ESI-MS/MS: 835.4162 $[M-Boc-CH_3(C{=}O)N+H]^+$, 809.4351 $[M-Boc-CH_3(C{=}O)N-CN+H]^+$.

*4.1.27. 2-({[5-(7-{[5-Amino-1-({[3′-(5-carbamimidoyl-1H-indol-2-yl)-4′-hydroxy-[1,1′-biphenyl]-4-yl]methyl}carbamoyl)pentyl] carbamoyl}heptanamido)-1-carboxypentyl]carbamoyl} amino) pentanedioic acid (**28**) and (Z)-4-(4-aminobutyl)-1-(4′-hydroxy-3′-(5-(N-(1-hydroxyethylidene)carbamimidoyl)-1H-indol-2-yl)-[1,1′-biphenyl]-4-yl)-3,6,13,21-tetraoxo-2,5,14,20,22-pentaazapentacosane-19,23,25-tricarboxylic acid (**29**)*

To a solution of compound **27** in a mixture of dioxane, water, and acetic acid (5 mL, 6:2:1) was added catalytic amount of Raney-nickel. The mixture was shaken under 50 psi of H_2 for 4 h. The mixture was filtered through Celite and the filtrate was concentrated to dryness under reduced pressure. The crude residue was purified by reversed-phase HPLC to afford a mixture of compounds **28** and **29**. HPLC: acetonitrile (A)/water (B) (0.1% formic acid). The gradient consisted of 10% A to 35% A over 8 min; 35% A to 10% A over 10 min at 2 mL/min flow rate, R_t = 8.36 min, Yield: 30%, HRMS (ESI) compound **28**: $[M-H]^-$ calcd for C48H63N9O11: 940.4647, found: 940.4680, HRMS (ESI) compound **29**: $[M-H]^-$ calcd for C50H65N9O12: 982.4753, found: 982.4783.

*4.1.28. 1-(5-{[5-({[3′-(5-Carbamimidoyl-1H-indol-2-yl)-4′-hydroxy-[1,1′-biphenyl]-4-yl] methylcarbamoyl)-5-{7-[(5-carboxy-5-{[(1,3-dicarboxypropyl)carbamoyl]amino}entyl) carbamoyl] heptanamido}pentyl]carbamoyl}pentyl)-3,3-dimethyl-2-[(E)-2-[(3E)-3-{2-[(2E)-1,3,3-trimethyl-5-sulfonato-2,3-dihydro-1H-indol-2-ylidene]ethylidene}cyclohex-1-en-1-yl]ethenyl]-3H-indol-1-ium-5-sulfonate (**30**) and 1-{5-[(5-{7-[(5-carboxy-5-{[(1,3-dicarboxypropyl)carbamoyl]amino}pentyl)carbamoyl] heptanamido}-5-({[4′-hydroxy-3′-(5-{[(Z)-(1-hydroxyethylidene) amino]methanimidoyl}-1H-indol-2-yl)-[1,1′-biphenyl]-4-yl]methyl} carbamoyl)pentyl)carbamoyl]pentyl}-3,3-dimethyl-2-[(E)-2-[(3E)-3-{2-[(2E)-1,3,3-trimethyl-5-sulfonato-2,3-dihydro-1H-indol-2-ylidene]ethylidene}cyclohex-1-en-1-yl]ethenyl]-3H-indol-1-ium-5-sulfonate (**31**)*

To a mixture of compounds **28** and **29** (2 mg in 0.3 mL of DMSO) were added Tris–HCl buffer (0.3 mL, 0.1 M, pH = 8.5) and Sulfo-Cyanine 7 NHS ester (2 mg in 0.1 mL of DMSO). The reaction mixture was stirred at room temperature for 4 h. The residue was purified by reversed-phase HPLC to afford compounds **30** and **31**, respectively. HPLC: mobile phase acetonitrile (A)/water (B) (0.1% formic acid). The gradient consisted of 30%–40% A over 20 min; 40%–30% A over 25 min at 3.5 mL/min flow rate, $R_t = 5.18$ min for **30**, 6.21 min for **31**. Yield: 37% (**30**), 45% (**31**), compound **30**: LRMS (ESI) $[M+H]^+$ calcd for C85H104N11O18S2: 1631.7 found: $[M+3H]^{3+}$ 544.8, $[M+2H]^{2+}$ 816.8, and $[M+H]^+$ 1631.7; HRMS (ESI): $[M+3H]^{3+}$ 545.3593, $[M+3Na]^{3+}$ 567.3402, ESI-MS/MS: 370.3259 [M-(Lys-urea-Glu)-2SO3-NH3-CN+3H]$^{3+}$, compound **31**: LRMS (ESI) $[M+H]^+$ calcd for C87H106N11O19S2: 1674.9, found: $[M+3H]^{3+}$ 558.8, $[M+2H]^{2+}$ 838.0 and $[M+H]^+$ 1674.7.

4.2. Biological evaluation

4.2.1. In vitro hepsin-inhibitory assay

The synthesized compounds (10 nM–10 μM) were diluted in 2% DMSO and mixed with activated hepsin (#4776-SE-010, R&D Systems, Minneapolis, Minnesota) to a 96-well plate (REF 353219; BD Falcon). The final assay concentration for hepsin was 0.3 nM in TNC buffer (25 mM Tris, 150 mM NaCl, 5 mM $CaCl_2$, 0.01% Triton X-100, pH 8). After incubation for 30 min at room temperature Boc-QAR-AMC substrate (#ES014, R&D Systems, Minneapolis, Minnesota) was added to the Hepsin assays. The final substrate concentration was 150 μM in final reaction volume of 100 μL. Changes in fluorescence (excitation at 380 nm and emission at 460 nm) were measured at room temperature over time in a Biotek Synergy 2 plate reader (Molecular devices). From a plot of the mean reaction velocity *versus* compound concentration, a non-linear four parameter curve fit was performed using GraphPad Prism version 4.03 for Windows (GraphPad Software, SanDiego, CA, www.graphpad.com) to determine inhibitor IC_{50}.

4.2.2. In vitro PSMA-inhibitory assay

The IC_{50} values of compounds **30** and **31** were measured using NAALADase assay where the glutamic acid/glutamate released from the natural substrate of PSMA was analyzed by the fluorescence-based Amplex Red Glutamic Acid/Glutamate Oxidase assay kit (Invitrogen). *In vitro* PSMA binding affinities of the synthesized compounds were evaluated by following the manufacturer's procedure (www.lifetechnologies.com). Briefly, in a 96-well half area black flat bottom polystyrene NBS microplate (Corning, Tewksbury, MA), PSMA (3 nM, 10 μL) and different concentrations of inhibitor (20 μL) or buffer (TBS, 20 μL) were incubated at 37 °C for 30 min. Then NAAG (4 μM, 10 μL) was added to the mixture (37 °C, 30 min). The fluorescence signals generated from the Amplex working solution (50 μL) with the NAAG-liberated glutamate (37 °C, 1 h) were then quantified by the Synergy H4 hybrid multi-mode microplate reader (excitation at 530 nm and emission at 590 nm). Data was analyzed by non-linear regression with GraphPad Prism 4.03 for Windows to determine inhibitor IC_{50}.

4.2.3. In vitro cell uptake study

PC3/ML, PC3/ML-HPN, PC3/ML-PSMA and PC3/ML-PSMA-HPN cells were prepared at Johns Hopkins Medical Institutions, Baltimore, Maryland. The cells were seeded at a density of 5×10^5 cells/well in 6-well plates for 48 h until total adhesion was achieved. Then the medium was removed, and **30** and **31** (final concentration: 10 μg/mL) in RPMI 1640 medium supplemented with 10% FBS were added. After another 4 h of incubation, the cells were washed with cold PBS twice and fixed with 4% paraformaldehyde for 10 min and the flow cytometry (LSRII, BD Biosciences, San Jose, CA) analysis was employed to estimate the cellular uptake at different cell lines. Data were processed by FlowJo software (Ashland, OR).

4.2.4. In vivo near infrared (NIR) optical imaging study

One million cells of PC3/ML-PSMA and PC3/ML-PSMA-HPN were subcutaneously injected into upper flanks of six-week old male NSG (NOD/Shi-*scid*/IL-2Rγ^{null}) mice. Two weeks after the cell injection, one nanomole of **30** in 100 μL of PBS was injected *via* tail vein. Images were taken 24 h post injection of **30** using the Pearl Impulse Small Animal Imaging System (LI-COR, Lincoln, NA).

4.3. In silico molecular docking studies

4.3.1. Ligand preparation and optimization

All ligands **13**–**21** were generated as 2D and 3D structure by ChemBioDraw (ver. 11.0.1) and Chem3D Pro (ver. 11.0.1), respectively. The prepared compounds and CA-14, the original crystal ligand of hepsin X-ray crystal structure (PDB ID: 1O5E), were saved as *.sdf* file. The process of ligand preparation and optimization was performed by '*Sanitize*' preparation protocol in *SYBYL-X 2.1.1* (Tripos Inc., St Louis) to clean up the structures involving filling valences, standardizing, removing duplicates and producing only one molecule per input structure.

4.3.2. Protein preparation

The hepsin structure of in PDB format was downloaded from RCSB protein data bank (PDB ID: 1O5E). Structure preparation tool in *SYBYL-X* 2.1.1 was employed for the protein preparation. The original crystal ligand and water molecules were removed from the protein-ligand complexes for docking. Conflicted side chains of amino acid residues were fixed. Hydrogen atoms were added under the application of *TRIPOS* Force Field as a default setting. Minimization process was performed by *POWELL* method, initial optimization option was changed to *None* from a default setting *SIMPLEX*, and termination gradient and max iteration were set 0.5 kcal/(mol Å) and 1000 times, respectively.

4.3.3. Molecular docking

Docking studies of all prepared ligands were performed by *Surflex-Dock Geom* module in *SYBYL-X 2.1.1*. Docking was guided by the *Surflex-Dock* protomol, an idealized representation of a ligand that makes every potential interaction with the binding site. The binding site of hepsin X-ray crystal structure (PDB ID: 1O5E) for *Surflex-Dock* was defined according to the location information of CA-14, the original ligand. Two factors related with a generation of Protomol are *Bloat* (Å) and *Threshold* were set to 0.5 and 0, respectively. The maximum number of generated poses per each ligand and the minimum RMSD between final poses were set to 20 and 0.05, respectively. Other parameters were applied with its default settings in all runs. The *Surflex-Dock* scoring function, which contains hydrophobic, polar, repulsive, entropic and solvation

terms, was trained to estimate the dissociation constant (K_d) expressed in −log (K_d) units. The docked poses were obtained after running *Surflex-Dock* and the scores of the docked poses were ranked according to total score and Cscore (Table 2: Supplementary data).

Acknowledgments

This research supported by the NIH (CA134675 and CA184228 to M.G.P), USA Department of Defense (W81XWH-10-1-0189 to Y.B), the National Research Foundation of Korea (NRF) (2014R1A1A2056522 and 2014R1A4A1007304 to Y.B).

Appendix A. Supplementary data

Supplementary data related to this article can be found at http://dx.doi.org/10.1016/j.ejmech.2016.04.033.

References

[1] R. Siegel, J. Ma, Z. Zou, A. Jemal, Cancer statistics, 2014, CA Cancer J. Clin. 64 (2014) 9–29.
[2] A. Horwich, C. Parker, C. Bangma, V. Kataja, E.G.W. Group, Prostate cancer: ESMO Clinical Practice Guidelines for diagnosis, treatment and follow-up, Ann. Oncol. 21 (Suppl. 5) (2010) v129–v133.
[3] M.E. Ford, S.L. Havstad, R. Demers, C. Cole Johnson, Effects of false-positive prostate cancer screening results on subsequent prostate cancer screening behavior, Cancer Epidemiol. Biomark. Prev. 14 (2005) 190–194.
[4] E.A.M. Heijnsdijk, E.M. Wever, A. Auvinen, J. Hugosson, S. Ciatto, V. Nelen, M. Kwiatkowski, A. Villers, A. Páez, S.M. Moss, M. Zappa, T.L.J. Tammela, T. Mäkinen, S. Carlsson, I.J. Korfage, M.-L. Essink-Bot, S.J. Otto, G. Draisma, C.H. Bangma, M.J. Roobol, F.H. Schröder, H.J. de Koning, Quality-of-life effects of prostate-specific antigen screening, New Engl. J. Med. 367 (2012) 595–605.
[5] F.H. Schröder, J. Hugosson, M.J. Roobol, T.L.J. Tammela, S. Ciatto, V. Nelen, M. Kwiatkowski, M. Lujan, H. Lilja, M. Zappa, L.J. Denis, F. Recker, A. Páez, L. Määttänen, C.H. Bangma, G. Aus, S. Carlsson, A. Villers, X. Rebillard, T. van der Kwast, P.M. Kujala, B.G. Blijenberg, U.-H. Stenman, A. Huber, K. Taari, M. Hakama, S.M. Moss, H.J. de Koning, A. Auvinen, Prostate-cancer mortality at 11 years of follow-up, New Engl. J. Med. 366 (2012) 981–990.
[6] A.J. Vickers, C. Till, C.M. Tangen, H. Lilja, I.M. Thompson, An empirical evaluation of guidelines on prostate-specific antigen velocity in prostate cancer detection, J. Natl. Cancer Inst. 103 (2011) 462–469.
[7] J. Wilbur, Prostate cancer screening: the continuing controversy, Am. Fam. Physician 78 (2008) 1377–1384.
[8] S.P. Rowe, K.L. Gage, S.F. Faraj, K.J. Macura, T.C. Cornish, N. Gonzalez-Roibon, G. Guner, E. Munari, A.W. Partin, C.P. Pavlovich, M. Han, H.B. Carter, T.J. Bivalacqua, A. Blackford, D. Holt, R.F. Dannals, G.J. Netto, M.A. Lodge, R.C. Mease, M.G. Pomper, S.Y. Cho, F-18-DCFBC PET/CT for PSMA-based detection and characterization of primary prostate cancer, J. Nucl. Med. 56 (2015) 1003–1010.
[9] X. Tang, S.S. Mahajan, L.T. Nguyen, F. Beliveau, R. Leduc, J.A. Simon, V. Vasioukhin, Targeted inhibition of cell-surface serine protease hepsin blocks prostate cancer bone metastasis, Oncotarget 5 (2014) 1352–1362.
[10] K.A. Kelly, S.R. Setlur, R. Ross, R. Anbazhagan, P. Waterman, M.A. Rubin, R. Weissleder, Detection of early prostate cancer using a hepsin-targeted imaging agent, Cancer Res. 68 (2008) 2286–2291.
[11] S.R. Banerjee, M. Pullambhatla, C.A. Foss, A. Falk, Y. Byun, S. Nimmagadda, R.C. Mease, M.G. Pomper, Effect of chelators on the pharmacokinetics of Tc-99m-labeled imaging agents for the prostate-specific membrane antigen (PSMA), J. Med. Chem. 56 (2013) 6108–6121.
[12] Y. Chen, M. Pullambhatla, C.A. Foss, Y. Byun, S. Nimmagadda, S. Senthamizhchelvan, G. Sgouros, R.C. Mease, M.G. Pomper, 2-(3-{1-Carboxy-5-[(6-[F-18]fluoro-pyridine-3-carbonyl)-amino]-pentyl}-ureido)-pentane-dioic acid, [F-18]DCFPyL, a PSMA-based PET imaging agent for prostate cancer, Clin. Cancer. Res. 17 (2011) 7645–7653.
[13] S.R. Banerjee, M. Pullambhatla, Y. Byun, S. Nimmagadda, G. Green, J.J. Fox, A. Horti, R.C. Mease, M.G. Pomper, Ga-68-labeled inhibitors of prostate-specific membrane antigen (PSMA) for imaging prostate cancer, J. Med. Chem. 53 (2010) 5333–5341.
[14] H.M. Shallal, I. Minn, S.R. Banerjee, A. Lisok, R.C. Mease, M.G. Pomper, Heterobivalent agents targeting PSMA and integrin-alphavbeta3, Bioconjug. Chem. 25 (2014) 393–405.
[15] A. Ghosh, W.D. Heston, Tumor target prostate specific membrane antigen (PSMA) and its regulation in prostate cancer, J. Cell. Biochem. 91 (2004) 528–539.
[16] S.R. Banerjee, C.A. Foss, M. Castanares, R.C. Mease, Y. Byun, J.J. Fox, J. Hilton, S.E. Lupold, A.P. Kozikowski, M.G. Pomper, Synthesis and evaluation of technetium-99m- and rhenium-labeled inhibitors of the prostate-specific membrane antigen (PSMA), J. Med. Chem. 51 (2008) 4504–4517.
[17] M.I. Davis, M.J. Bennett, L.M. Thomas, P.J. Bjorkman, Crystal structure of prostate-specific membrane antigen, a tumor marker and peptidase, Proc. Natl. Acad. Sci. U. S. A. 102 (2005) 5981–5986.
[18] J.R. Somoza, J.D. Ho, C. Luong, M. Ghate, P.A. Sprengeler, K. Mortara, W.D. Shrader, D. Sperandio, H. Chan, M.E. McGrath, B.A. Katz, The structure of the extracellular region of human hepsin reveals a serine protease domain and a novel scavenger receptor cysteine-rich (SRCR) domain, Structure 11 (2003) 1123–1131.
[19] S.M. Dhanasekaran, T.R. Barrette, D. Ghosh, R. Shah, S. Varambally, K. Kurachi, K.J. Pienta, M.A. Rubin, A.M. Chinnaiyan, Delineation of prognostic biomarkers in prostate cancer, Nature 412 (2001) 822–826.
[20] O. Klezovitch, J. Chevillet, J. Mirosevich, R.L. Roberts, R.J. Matusik, V. Vasioukhin, Hepsin promotes prostate cancer progression and metastasis, Cancer Cell 6 (2004) 185–195.
[21] K.A. Landers, M.J. Burger, M.A. Tebay, D.M. Purdie, B. Scells, H. Samaratunga, M.F. Lavin, R.A. Gardiner, Use of multiple biomarkers for a molecular diagnosis of prostate cancer, Int. J. Cancer 114 (2005) 950–956.
[22] V.N. Talesa, C. Antognelli, C. Del Buono, F. Stracci, M.R. Serva, E. Cottini, E. Mearini, Diagnostic potential in prostate cancer of a panel of urinary molecular tumor markers, Cancer Biomark. 5 (2009) 241–251.
[23] M. Eder, M. Schafer, U. Bauder-Wust, U. Haberkorn, M. Eisenhut, K. Kopka, Preclinical evaluation of a bispecific low-molecular heterodimer targeting both PSMA and GRPR for improved PET imaging and therapy of prostate cancer, Prostate 74 (2014) 659–668.
[24] B.A. Katz, C. Luong, J.D. Ho, J.R. Somoza, E. Gjerstad, J. Tang, S.R. Williams, E. Verner, R.L. Mackman, W.B. Young, P.A. Sprengeler, H. Chan, K. Mortara, J.W. Janc, M.E. McGrath, Dissecting and designing inhibitor selectivity determinants at the S1 site using an artificial Ala190 protease (Ala190 uPA), J. Mol. Biol. 344 (2004) 527–547.
[25] M. Subedi, J. Chen, E. Kang, K.I. Kim, Y. Byun, Facile synthesis of 2-(4-hydroxybiphenyl-3-yl)-1H-indoles from anilines and 5′-bromo-2′-hydroxyacetophenone, Synth. Commun. 45 (2015) 1704–1709.
[26] J.H. Forsberg, V.T. Spaziano, T.M. Balasubramanian, G.K. Liu, S.A. Kinsley, C.A. Duckworth, J.J. Poteruca, P.S. Brown, J.L. Miller, Use of lanthanide(III) ions as catalysts for the reactions of amines with nitriles, J. Org. Chem. 52 (1987) 1017–1021.
[27] R.A. Moss, W. Ma, D.C. Merrer, S. Xue, Conversion of 'obstinate' nitriles to amidines by Garigipati's reaction, Tetrahedron Lett. 36 (1995) 8761–8764.
[28] S. Chandrappa, H. Chandru, A.C. Sharada, K. Vinaya, C.S. Ananda Kumar, N.R. Thimmegowda, P. Nagegowda, M. Karuna Kumar, K.S. Rangappa, Synthesis and in vivo anticancer and antiangiogenic effects of novel thioxothiazolidin-4-one derivatives against transplantable mouse tumor, Med. Chem. Res. 19 (2010) 236–249.
[29] M.L. Quan, P.C. Wong, C. Wang, F. Woerner, J.M. Smallheer, F.A. Barbera, J.M. Bozarth, R.L. Brown, M.R. Harpel, J.M. Luettgen, P.E. Morin, T. Peterson, V. Ramamurthy, A.R. Rendina, K.A. Rossi, C.A. Watson, A. Wei, G. Zhang, D. Seiffert, R.R. Wexler, Tetrahydroquinoline derivatives as potent and selective factor XIa inhibitors, J. Med. Chem. 57 (2014) 955–969.
[30] K.P. Maresca, S.M. Hillier, F.J. Femia, D. Keith, C. Barone, J.L. Joyal, C.N. Zimmerman, A.P. Kozikowski, J.A. Barrett, W.C. Eckelman, J.W. Babich, A series of halogenated heterodimeric inhibitors of prostate specific membrane antigen (PSMA) as radiolabeled probes for targeting prostate cancer, J. Med. Chem. 52 (2009) 347–357.
[31] R.L. Mackman, B.A. Katz, J.G. Breitenbucher, H.C. Hui, E. Verner, C. Luong, L. Liu, P.A. Sprengeler, Exploiting subsite S1 of trypsin-like serine proteases for selectivity: potent and selective inhibitors of urokinase-type plasminogen activator, J. Med. Chem. 44 (2001) 3856–3871.
[32] Y. Chen, S. Dhara, S.R. Banerjee, Y. Byun, M. Pullambhatla, R.C. Mease, M.G. Pomper, A low molecular weight PSMA-based fluorescent imaging agent for cancer, Biochem. Biophys. Res. Commun. 390 (2009) 624–629.